J. CHEM. SOC. FARADAY TRANS., 1995, 91(17), 2899–2905

Oxydehydrogenation of Propane on V_2O_5/TiO_2 Catalyst: Kinetic and Mechanistic Aspects

Nathalie Boisdron, Agnès Monnier, Louise Jalowiecki-Duhamel* and Yolande Barbaux
Laboratoire de Catalyse Hétérogène et Homogène, U.R.A. C.N.R.S. D04020, Bât C3, Université des Sciences et Technologies de Lille, 59655 Villeneuve d'Ascq Cedex, France

Catalytic oxydehydrogenation of propane and work function measurements in similar conditions have been performed on V_2O_5/TiO_2 catalyst. The oxidation mechanism $C_3H_8 \xrightarrow{k_1} C_3H_6 \xrightarrow{k_2} CO_x + H_2O$ has been kinetically modelled which permits theoretical evolution of the selectivity as a function of the conversion, for various ratios of $K = k_1/k_2$. A good correlation is obtained between the experimental and theoretical curves, validating the kinetic modelling. The value obtained for K is $\ll 1$, so the reactivity of propene is much higher than that of propane and justifies the observed yield limitation. Moreover, the rate-determining step of propane ODH reaction as well as of propene oxidation is attributed to the attack of the oxidized site by the hydrocarbon. The value of K, which depends on the type of catalyst may be used to evaluate the selectivity to propene and for classification of oxydehydrogenation catalysts. The work function measurements give the nature and charge of the various oxygen species (O_2^-, O^-, O^{2-}) involved in the reaction, and O^{2-} is found to react with propane.

1. Introduction

Activation and functionalization of alkanes is an important process from both an industrial and a fundamental point of view. For propane and *n*-butane dehydrogenation, typical oxidation catalysts are vanadium-based compounds,[1–6] but some bismuth, cobalt and nickel molybdates,[7–9] have also been proposed as active and selective catalysts. Over the years, various proposals have been forwarded to explain the changes in selectivity and yields for different reactions over various catalysts.[10–13] But none of the proposals is satisfactory in terms of being able to explain all available data. This is probably because of the very different conditions under which the data were collected. Therefore, a classification of the various catalytic systems is not easy, because of the numerous parameters able to influence the results obtained, even on the same compound. Nevertheless, the best yields for the transformation of propane,[2,5,9,14] are still low.

The detailed mechanism and the characteristics of active centres is still unclear. However, it is apparent that the observed product distribution depends not only on the nature of the catalyst but also on the nature of the alkane,[1–3,13–21] even if there exist some common features such as breakage of the C—H bond, which appears to be the rate-determining step.[18] In the case of oxydehydrogenation (ODH) of propane much detailed work has concerned the V—Mg—O system and the relation between the performance of the catalysts and the type of vanadium species present;[2,3,13,21–23] only a few publications present kinetic data.[23]

In the present work, we intend to elucidate further the mechanism of oxydehydrogenation of propane, and its possible influence on yield limitation, with the aim to compare and classify the various catalytic systems. Work function measurements in parallel with the catalytic tests permit us not only to reach this goal but also to identify the charge of the reactive oxygen species on the catalytic surface. This aspect needs to be studied further because there is no general consensus about the role of lattice and gas-phase oxygen in selective and complete oxidation reactions of C_4 hydrocarbons.[24] In addition, no studies have been made concerning its role in C_3 oxydehydrogenation.

2. Experimental

V_2O_5/TiO_2 containing four monolayers of V_2O_5 on TiO_2 anatase (Prolabo, 8.7 m^2 g^{-1}, 1 monolayer corresponds to 10 V nm^{-2}) was prepared by impregnation with NH_4VO_3 (Labosi, 99%), dried overnight at 130 °C and calcined in a stream of air at 550 °C for 4 h. Its specific surface area measured with the BET method was 6.6 m^2 g^{-1}.

The catalytic oxidation of C_3H_8 was performed under atmospheric pressure by co-feeding the nitrogen-diluted reaction gases ($C_3H_8 : O_2 : N_2 = 5 : 15 : 80$). The total flow rate was 50 ml min^{-1} (down flow), the reaction temperature was in the range 350–500 °C, and the catalyst mass was 1.64 g (velocity vapour hourly, VVH : 2000). The catalyst was tested in a fixed-bed stainless-steel tubular reactor (length 300 mm, internal diameter 15 mm) equipped with a coaxial thermocouple for temperature profiling. All the gases were purified on-line by the use of filters. Prior to this, the reaction mixture was homogenized with a heat vaporizer (120–200 °C). The precatalytic region was filled with fine quartz chips (0.8 mm $< \phi <$ 1.6 mm) to minimize contributions due to gas-phase reaction. The catalyst powder was supported by quartz wool maintained by an inox grid. It was verified that under these conditions there was little gas-phase reaction in the absence of the catalyst. A thermocouple was placed in the centre of the catalyst bed in order to check the temperature. After reaction, the tubings were heated to prevent condensation of products.

Propene, CO_2 and CO were the main reaction products, they were sampled on-line using an automatic sampling valve (Valco) and analysed by on-line gas chromatography (Shimadzu GC 9-A). Two lines of analysis were used in parallel and simultaneously, with a programmation of temperature of the columns (55 °C for 7.7 min, then 30 °C min^{-1} up to 70 °C, and finally 18 min at 70 °C). On each analysis line, two columns were used: (Ii) Porapak R (2.50 m, 80/100, 1/8″), (Iii) molecular sieve [5 Å, 2.50 m, 60/80, 1/8″ (1″ = 2.54 cm)], connected to a thermal conductivity detector, helium was the carrier gas (35 ml min^{-1}); (IIi) XOB 0.75/spherosil (0.6 m, 1/8″), (IIii) squalane 10%/porasil C (2.50 m, 80/100, 1/8″), connected to a flame ionization detector, helium was the carrier gas (10 ml min^{-1}). The amount of oxygenates (acetic acid, acrolein, acrylic acid *etc.*) not exceeding 2% was analysed separately by gas chromatography (Delsi 700) using a semi-capillary column (OV 351, 30 m, 0.53 mm) with a temperature programme of 40 °C for 1 min and then 10 °C min^{-1} up to 190 °C and a flame ionization detector; the carrier gas was helium.

The work function of the samples was measured by the vibrating condenser (Kelvin) method. The method involves recording the Volta potential difference ΔV between two plates of a condenser made of the sample and the reference electrode. ΔV is equal to the difference in the work functions of the solids which form the two plates of the condenser. As the work function of the reference electrode is constant under the experimental conditions adopted, the variations in ΔV reflect the changes in the work function of the sample. In the cases in which the structure of the bulk of the solids is not changed by chemisorption of gases or surface doping, the work function is a measure of the surface potential, defined as the difference between the electrostatic potential at the surface immediately outside a solid and the internal electric potential. The surface potential represents a potential barrier which as to be surmounted by an electron distribution in the surface layer and depends on the dipole structure of the solid surface.

The apparatus used in the present work consisted of a stainless-steel cell containing two electrodes mounted vertically. The potential measuring cell was connected to a gas-flow system which allowed controlled streams of oxygen and/or hydrocarbons (C_1–C_3) and the measurements were performed in the temperature range 50–500 °C. Further details of the measurements have been reported elsewhere.[25] The sample electrode was constructed of a stainless-steel plate 20 mm × 30 mm and 1.5 mm thick, covered on one side with gold foil, on which a sample of the powder under study was deposited from a suspension in amyl alcohol. The heating Thermocoax element and thermocouple for recording the sample temperature were placed inside the steel plate. The vibrating reference electrode facing the sample electrode at a distance of 1 mm was made of a graphite plate 3 mm thick. The choice of reference electrode was a subject of a separate paper.[26]

The work function of the reference electrode was constant under measurement conditions. The values of surface potential, reported in the text are relative to the graphite electrode potential: $V = V_{\text{graphite}} - V_{\text{sample}}$, an increase of the value of the potential difference indicates that the surface becomes more negatively charged. The surface potentials were reproducible for a given sample within 5 mV.

3. Results and Discussion

3.1 Catalytic Activity

Fig. 1 presents the selectivity to propene as a function of total conversion of C_3H_8 at 450 °C for the studied catalyst. The selectivity decreases when the conversion increases and the propene yield presents a maximum. Therefore, a consecutive reaction mechanism is envisaged. But, in order to be able to propose a kinetic model, the effect on propane ODH reaction and on propene oxidation of the partial pressure of the various reactants (propane, O_2), was studied first.

3.1.1 *Influence of Partial Pressures*

The reaction rates of propane ODH reaction and propene oxidation can be written as follows:

$$v = kP_{\text{HC}}^{\alpha}P_{\text{O}_2}^{\beta}$$

α and β, are respectively the hydrocarbon and oxygen partial orders for the reactions.

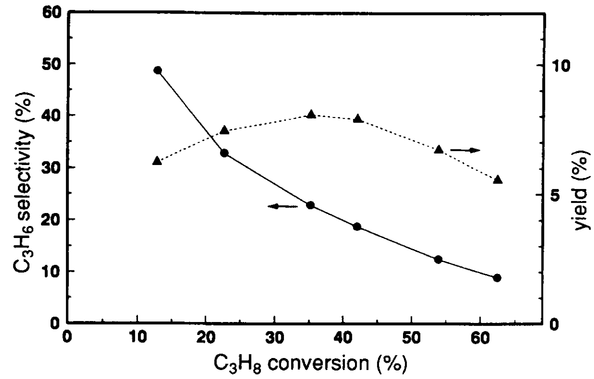

Fig. 1 Selectivity to propene or yield as a function of total conversion of propane at 450 °C on V_2O_5/TiO_2

The experimental conditions applied to determine the hydrocarbon and oxygen partial orders α and β are summarized in Table 1. The catalytic experiments were performed at constant contact time for propane and propene. The catalytic mass was 0.50 g and the reaction temperature was varied (473 K for propane ODH and 347 K for propene oxidation) in order to achieve a hydrocarbon conversion of *ca.* 10–15%.

The propane and propene disappearance rates (v) can be measured, and therefore the partial orders are obtained by plotting the logarithm of v as a function of the logarithm of the partial pressures of hydrocarbon and oxygen. The results obtained are reported in Table 2.

For propane ODH, only the partial pressure of hydrocarbon ($\alpha = 1$) really has an influence on the catalytic reaction, whereas the partial pressure of oxygen has almost no effect ($\beta = 0$). Nevertheless, one must remark, that for propene oxidation, the value found for β is very close to zero but a little higher and the oxygen pressure could have a small effect on propene oxidation. The important result is that for the two reactions (propane ODH and propene oxidation) the rate-determining step corresponds to the attack of the catalytic surface by the hydrocarbon, in agreement with the results published by Andersson.[23]

3.1.2 *Kinetic Model*

A consecutive reaction mechanism can be written as follows:

$$C_3H_8 \xrightarrow{k_1} C_3H_6 \xrightarrow{k_2} CO_x + H_2O$$

Table 1 Experimental conditions applied to determine the hydrocarbon and oxygen partial orders according to the equation $v = kP_{\text{HC}}^{\alpha}P_{\text{O}_2}^{\beta}$

order	reactant	propane ODH	propene oxidation
α	HC%	2.5–12.5[a]	2.5–12.5[a]
	O_2%	50	50
β	HC%	5	5
	O_2%	10–50[a]	10–50[a]

P_{HC} = partial pressure of hydrocarbon; P_{O_2} = partial pressure of oxygen; [a] pressure ranges.

Table 2 Hydrocarbon and oxygen partial orders according to the equation $v = kP_{\text{HC}}^{\alpha}P_{\text{O}_2}^{\beta}$

order	propane ODH	propene oxidation
α	1.05	0.91
β	~0	0.09

P_{HC} = partial pressure of hydrocarbon and P_{O_2} = partial pressure of oxygen.

For non-porous catalysts and first-order reactions, the yield in intermediate products (propene) leads to a set of differential equations:

$$-\frac{dP_{C_3H_8}}{dt} = k_1 P_{C_3H_8} \qquad (1)$$

$$\frac{dP_{C_3H_6}}{dt} = k_1 P_{C_3H_8} - k_2 P_{C_3H_6} \qquad (2)$$

where $P_{C_3H_8}$ and $P_{C_3H_6}$ are, respectively, the partial pressures of propane and propene. By dividing eqn. (2) by eqn. (1), the following result is obtained:

$$-\frac{dP_{C_3H_6}}{dP_{C_3H_8}} = 1 - \frac{1}{K}\frac{P_{C_3H_6}}{P_{C_3H_8}} \qquad (3)$$

K is the selectivity factor ($K = k_1/k_2$). Integration of the above equations gives the selectivity in propene (S) as a function of the conversion of propane (C) when the total flow rate is constant:

$$S = \frac{K}{(K-1)}\frac{(1-C)}{C}[(1-C)^{-[1-(1/K)]} - 1] \qquad (4)$$

With $S = B/(A_{\text{initial}} - A_{\text{final}})$ and $C = (A_{\text{initial}} - A_{\text{final}})/A_{\text{initial}}$ (if $A = P_{C_3H_8}$ and $B = P_{C_3H_6}$)

The theoretical curves describing yield or selectivity as a function of conversion can be obtained and are presented in Fig. 2 for different values of K (0.1, 0.5, and 2). Considering the shape of the theoretical curves, one can see that the experimental results usually concern values of K much lower than 0.5 and of the order of 0.1.

For each experimental result (selectivity–conversion) a value of K can be calculated using eqn. (4), and the results obtained are presented in Table 3. For conversion values higher than *ca.* 35%, the value of K is equal to 0.12, increasing slowly up to a value of 0.13. For conversion values lower than 35%, the value of K increases slightly with the conversion, showing that the kinetic model is not completely in accord with the experimental results obtained. Nevertheless, quite a good correlation between experimental results and theoretical modelling is obtained. In Fig. 3 is shown the slight difference which exists between the experimental results and the theoretical curve, obtained from eqn. (4) with $K = 0.12$.

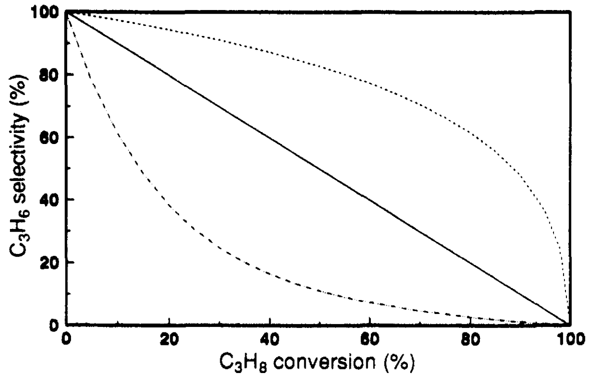

Fig. 2 Theoretical selectivity curves as a function of conversion for different values of K: 0.1 – · –; 0.5 ——; 2 – – –

Table 3 Calculated values of K (k_1/k_2) for each conversion–selectivity couple

conversion (%)	selectivity (%)	K
12.8	48.7	0.084
22.6	32.8	0.095
35.1	22.9	0.114
41.9	18.8	0.122
53.8	12.5	0.127
62.4	8.9	0.129

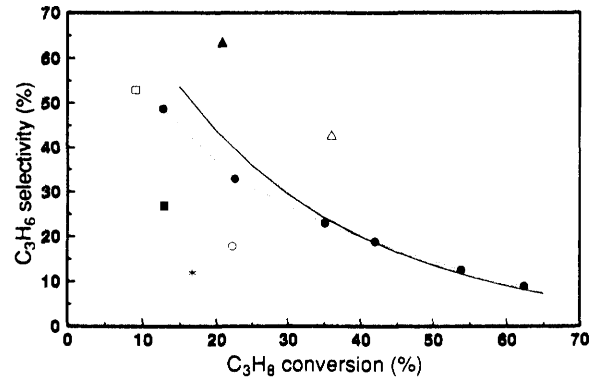

Fig. 3 Selectivity to propene as a function of conversion on V_2O_5/TiO_2: experimental (●) and theoretical —— ($K = 0.12$) curves; and on various compounds presented in the literature: ○, V_2O_5 (ref. 2); □, V_2O_5 (ref. 3); △, V—Mg—O (ref. 2); ■, V—Ti—O (ref. 22); ——, V—Ti—O (ref. 22); *, V—Si—O (ref. 22); ▲, Ni molybdate (ref. 9)

The variation of the value of K as a function of the conversion shows that the propane and propene oxidation rates ratio is not constant on the whole range of conversions. Such a phenomenon can be due to a too simple kinetic model which does not take into account: (i) all the reactions (formation of CO_x by a parallel route for instance); (ii) the diffusion processes; (iii) the change of the catalytic surface with the conversion; (iv) the mechanism for the adsorption of propane or propene to the surface of the catalyst. The last point could be important since the rate-determining step corresponds to the attack of the catalytic surface by the hydrocarbon. Nevertheless, this simple kinetic model gives an estimate of the ratio between the propane selective oxidation rate and the propene degradation rate. When $K = 0.12$, propene disappears eight times faster than propane. In general, the shape of curves presenting selectivity as a function of conversion that is usually observed in the literature corresponds to values for K much lower than 1 (Fig. 2); so the reactivity of propene is much higher than that of propane, which explains the difficulty in obtaining high yields in propene and, therefore, the yield limitation often observed in propane oxidation.

The value of K corresponds to a performance in selectivity; it depends on the solid and leads to a possible classification of oxydehydrogenation catalysts. Such a kinetic model has been verified on a different catalyst, $VOSO_4$. In Fig. 3 some published results on different systems are given for comparison with the present results. The Ni molybdate system and the V—Mg—O catalyst present much higher selectivities than the supported V_2O_5 systems and are for the moment the best catalysts presented in the literature for propane oxydehydrogenation leading to propene. It seems that these systems could be represented by the same selectivity–conversion curve leading to a rather similar value for K. Considering only a couple of points, conversion–selectivity may be insufficient to classify a catalyst, because at low conversions the determination of K presents an uncertainty. Nevertheless, for high conversions (>30%) a rather good classification can be obtained.

3.2 Work Function Measurements

3.2.1 *Work Function Measurements under Various Atmospheres*

For a given temperature (475 °C), the work function has been measured on V_2O_5/TiO_2 (Table 4). For the oxidized state (Ar–O_2) the potential is 1336 mV, whereas for the reduced state of the catalyst (Ar–hydrocarbon), the lowest value is obtained with propene (−140 mV) so the catalyst is more reduced with propene than with propane. Under the reaction mixture (O_2–Ar–hydrocarbon), the potential values obtained are very close to the potential value of the oxidized state, which means that the catalyst surface is only slightly reduced by the catalytic reaction and that the number of oxidized sites available for the catalytic reaction is very high. The work function results are therefore in good agreement with the catalytic tests because an oxygen partial order of zero has been obtained for propane and propene showing that the rate-determining step of the ODH reaction corresponds to the attack of the catalytic surface by the hydrocarbon.

Under O_2–Ar and for temperatures between 300 and 500 °C, the influence of the temperature on the potential value (1.33–1.34 V) is almost negligible. The variation of the potential value under the reaction mixture are much larger and are presented in Fig. 4. Nevertheless, the potential value under propene is always lower than the value under propane, for the range of temperatures studied (300–500 °C). So, under the reaction mixture the catalyst is always a little more reduced when the mixture contains propene rather than propane. For mixtures containing a hydrocarbon, the potential value increases as a function of temperature, which indicates that the activation energy of the oxidation of the sites is higher than the activation energy of the reduction of the sites.

3.2.2 *Under a Hydrocarbon Atmosphere Correlation with the Kinetic Model*

In the absence of gaseous oxygen, under a hydrocarbon atmosphere, the work function varies as a function of time; when the surface is saturated with adsorbed oxygen, the hydrocarbons react rapidly, depending on the temperature. As an example, Fig. 5 presents the work function evolution measured on V_2O_5/TiO_2 under a C_3H_6 atmosphere (5%) at 300 °C. The introduction of propane or propene in the argon flow leads to a work function decrease corresponding to a reduction of the oxidized sites (S_O) by a hydrocarbon

$$S_O + HC \rightarrow \text{products} + S_R$$

where S_O and S_R are the superficial sites, respectively, oxidized and reduced.

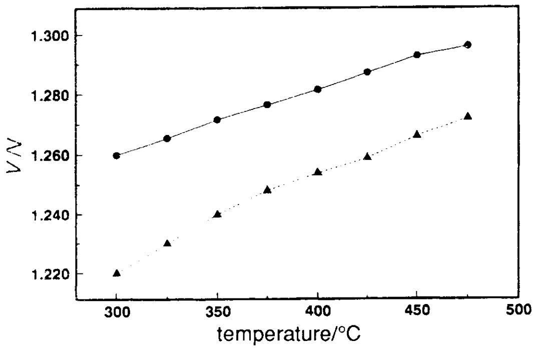

Fig. 4 Potential value variation under reaction mixture (5% hydrocarbon 54% oxygen) as a function of temperature (the hydrocarbon is ● C_3H_8, and ▲ C_3H_6)

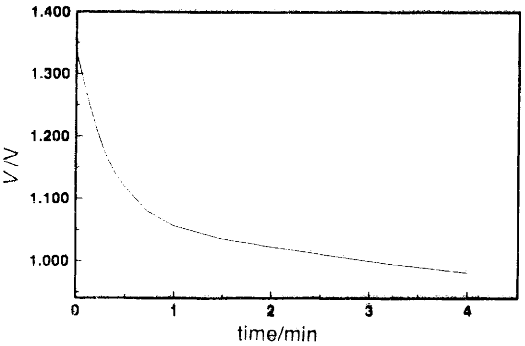

Fig. 5 Potential value variation under propene flow at 300 °C as a function of time

The work function decreases as a function of time but finally reaches a constant value, V_∞, corresponding to a disappearance of the oxidized sites (Fig. 6). The work function evolution as a function of time can be described by the following equations:

$$-\frac{d(S_O)}{dt} = -\frac{dV}{dt} = k'(V_\infty - V)P_{HC} \qquad (1)$$

where V_∞ is the work function value in the absence of adsorbed oxygen species on the surface (reduced state), and V_O is the work function measured at the initial state (oxidized state). At a potential V, $V - V_\infty$ corresponds to the number of oxidized sites and $V_O - V$ to the number of reduced sites.

dV/dt can be obtained directly by plotting the tangent at a constant potential V (Fig. 6); therefore, at V_O the initial rates are measured for each hydrocarbon [$v(C_3H_8)$, $v(C_3H_6)$]. Then, the ratio between the propane and propene reducing rates of the oxidized sites [$R = v(C_3H_8)/v(C_3H_6)$] can be determined from the work function measurements (Table 5).

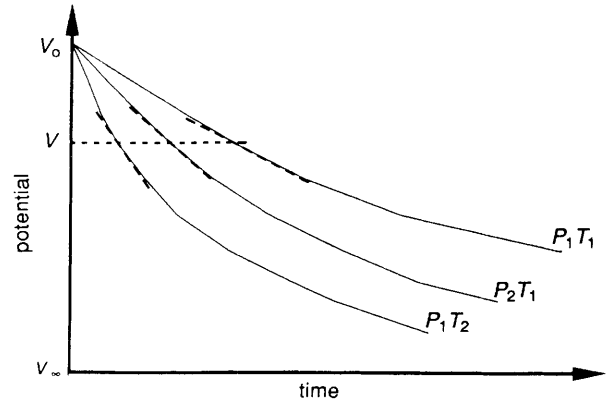

Fig. 6 Example of potential variation as a function of time for various pressures (P_1, P_2...) and temperatures (T_1, T_2...). V_∞ is the work function value in the absence of adsorbed oxygen species on the surface (reduced state), whereas V_O is the work function measured at the initial state (oxidized state).

Table 4 Surface potential values obtained at 475 °C under various atmospheres

gas phase/atm	O_2–Ar 0.16 : 0.84	O_2–Ar–C_3H_8 0.54 : 0.41 : 0.05	O_2–Ar–C_3H_6 0.54 : 0.41 : 0.05	Ar–C_3H_8 0.94 : 0.06	Ar–C_3H_6 0.94 : 0.06
potential at 475 °C/mV	1336	1296	1272	−68	−140

Table 5 Ratio between the propane and propene reducing rate obtained from work function measurements (at constant potential V and constant partial pressures of hydrocarbons)

$T/°C$	$R = v(C_3H_8)/v(C_3H_6)$
300	0.078
335	0.098
375	0.123
425	0.122
475	0.153

At 425 °C the rate $R = 0.12$ clearly shows that propene is more reactive than propane. So, work function measurements also confirm the much higher reactivity of propene. Moreover, the ratio R between the reducing power of propane and propene corresponds [at constant potential V and constant hydrocarbon pressure (5%)] to the ratio between the kinetic constant k'_1/k'_2 [eqn. (1')]:

$$-\frac{dV_1}{dt} = k'_1(V_\infty - V)P_{C_3H_8}$$

$$-\frac{dV_2}{dt} = k'_2(V_\infty - V)P_{C_3H_6}$$

Therefore, a good correlation is obtained between the work function measurements and the catalytic experiments; the value found for $R(k'_1/k'_2)$ is of the same order as the ratio determined by the use of the kinetic model (k_1/k_2).

For a constant potential V and varying temperature (Fig. 6), the activation energy of the reduction step can be determined from the slope of the straight lines obtained by plotting $\ln(dV/dt)$ as a function of $1/T$ (Fig. 7; Arrhenius plots). The activation energies obtained, respectively, for reduction with propane and propene are 9.6 kcal mol^{-1} and 6.5 kcal mol^{-1}. The values of the apparent activation energies for propane or propene determined by catalytic experiments (reporting ln v as a function of $1/T$) are very similar to each other; no difference is detectable between the selectivities for the propane ODH reaction. The apparent activation energy obtained for the total reaction is 14.7 kcal mol^{-1} (Fig. 8). A rather good correlation is obtained between the two techniques even if the activation energies determined by work function measurements are lower. These values remain rather similar and correspond to elementary steps, whereas those obtained by catalytic experiment correspond to an apparent energy of the overall propane conversion.

3.2.3 *Nature and Charge of the Reactive Oxygen Species*

Oxygen Atmosphere. The work function measurements permit the nature and charge to be determined of the various oxygen species (O_2^-, O^-, O^{2-}) involved in the reaction. The work function measurements under an oxygen–argon mixture ($P_{O_2} = 0.05$ atm) were performed in the temperature range 50–500 °C on V_2O_5/TiO_2 (anatase) and previously published.[27] Different temperature regions are observed where the potential values are fairly constant or presenting small variations: <100 °C, 100–380 °C, and >380 °C. Between these regions, the work function increases rapidly, the surface becoming more negative with the temperature.

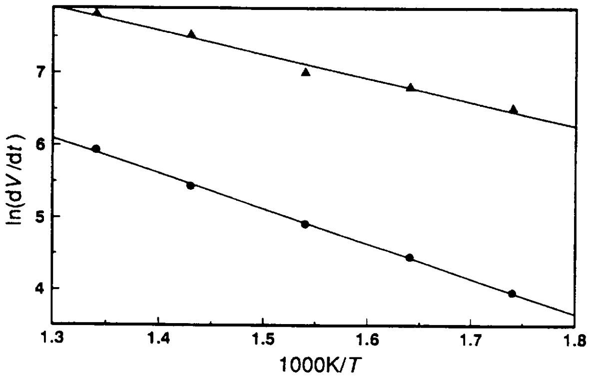

Fig. 7 Arrhenius plots for propane ● and ▲ propene reactions (results obtained from work function measurements)

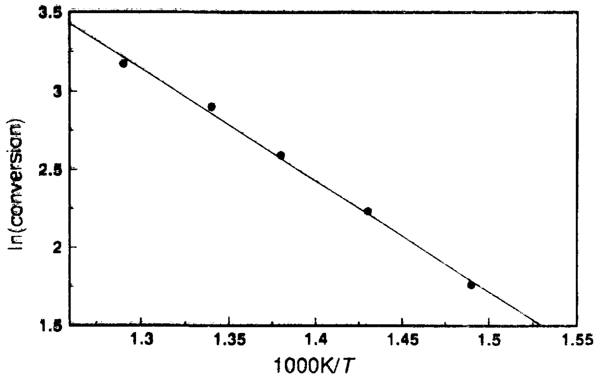

Fig. 8 Arrhenius plot for propane conversion (results obtained from catalytic experiments)

On the surface, an equilibrium exists between the adsorbed oxygen species and gaseous oxygen:[28]

$$O_2 + ne^- \Leftrightarrow O_{2(ads)}{}^{n-}$$

The mass action law is

$$K = \frac{(O_2{}^{n-})}{P_{O_2}\exp(-neV/k_B T)}$$

where k_B is Boltzmann's constant, T is the absolute temperature, e the electron charge and n the number of electrons transferred from the solid to the adsorbed species during the sorption process. From this equation, a relation between the work function value and the partial pressure of O_2 can be obtained:

$$V = \frac{k_B T}{ne}\ln P_{O_2} + \text{constant}$$

The value of n depends on the equilibrium between the gaseous molecule and the adsorbed oxygen species. The possibilities are:

$$n = 1 \quad O_2 + e^- \Leftrightarrow O_{2(ads)}{}^-$$

$$n = 2 \quad O_2 + 2e^- \Leftrightarrow 2O_{(ads)}{}^-$$

$$n = 4 \quad O_2 + 4e^- \Leftrightarrow 2O_{(ads)}{}^{2-}$$

The slope of the straight lines obtained by plotting the potential value V *vs.* the logarithm of the partial pressure of oxygen at a given temperature, leads to the value of n and therefore to the nature of the adsorbed oxygen species. O^- appears to be the dominant species within the 100–380 °C temperature range, the O_2^- species is found to exist for lower temperatures, whereas for temperatures higher than 385 °C the O^{2-} species are present on the surface (Table 6).

Interaction between Hydrocarbons and Oxygen Species. The work function values depend on the oxygen species concentration, therefore, the kinetic parameters of the reaction between any hydrocarbon and these active species can be determined as follows:

Table 6 Charge of the reactive oxygen species involved under O_2

T/°C	n	oxygen species
<100	1	O_2^-
100–380	2	O^-
>380	4	O^{2-}

hypothesis (1) reactive species O^-

$$O_2 + 2e^- \xrightarrow{k_1} 2O^-$$

$$O^- + HC \xrightarrow{k_2} \text{products} + e^-$$

oxidation rate is

$$v_{ox} = k_1 P_{O_2} \exp\left(-\frac{2eV}{k_B T}\right)$$

reduction rate is

$$v_{red} = k_2 P_{HC}[O^-]$$

at the steady state:

$$v_{red} = 2v_{ox}$$

$$\frac{2eV}{k_B T} = \ln \frac{k_1 P_{O_2}}{k_2 P_{HC}} + \ln \frac{2}{[O^-]}$$

$$V = \frac{k_B T}{2e} \ln \frac{P_{O_2}}{P_{HC}} + \text{constant}$$

hypothesis (2), reactive species O^{2-}

$$O_2 + 4e^- \xrightarrow{k_1} 2O^{2-}$$

$$O^{2-} + HC \longrightarrow \text{products} + 2e^-$$

variation of potential V:

$$V = \frac{k_B T}{4e} \ln \frac{P_{O_2}}{P_{HC}} + \text{constant}$$

The active oxygen species involved in the reaction mechansim can be deduced from the slope of the curve presenting the variation of the potential value V *vs.* the logarithm of the partial pressure of the reactants [Fig. 9(a) and (b)]. It has been presented previously (Table 6) that the O^{2-} species is found to be in equilibrium with the O_2 gas phase for temperatures higher than 380 °C. This equilibrium is affected by the presence of hydrocarbons and depending on the hydrocarbons present, various oxygen species are involved (Table 7).

At 425 °C, it is found that the O^{2-} species reacts with propane whereas O^- reacts with propene. Mazzochia *et al.* have already proposed that propene is formed by the reaction of propane with surface O^{2-} species on $NiMoO_4$ (ref. 29). Propane reacting with O^{2-} species, is in agreement with a heterolytic rupture of propane (with abstraction of a hydrogen atom) involving an O^{2-} species in a low coordination site. It has been often proposed that in the selective oxidation of hydrocarbons, the lattice oxygen of transition-metal oxides is responsible for hydrogen abstraction.[30] Bielanski and Haber postulated that O^{2-} should preferentially lead to partial oxidation,[31] confirmed on V_2O_5/TiO_2 (ref. 27) as well as on $Bi_2Mo_3O_{12}$ systems,[25] nevertheless the nature and charge of the reactive species is still controversial and sometimes it is assumed that O^{2-} is responsible for total oxidation.[32] Applying the experimental conditions presented in Table 7, the result obtained by work function measurements is that propene can react with O^-. These experimental conditions are as close as possible to the conditions found under catalytic testing but not exactly the same. Under catalytic conditions, propene is a reaction product and its partial pressure is <0.03 atm so one cannot eliminate the possibility that under catalytic conditions propene can react with an O^{2-} species. Such experimental conditions could not be applied because of the total conversion of oxygen in such a case. And so, under catalytic conditions (*i.e.* in the mixture of reactants and products) and for specific gas pressure, it is not impossible that the alkene can also react with an O^{2-} species. Therefore, in the case of heterogeneous limitation, each C_3 hydrocarbon should compete for the active site and react with the oxygen species. Considering the high reactivity of propene, a propene yield limitation should be observed with an increase of propane conversion.

Table 7 Charge of the reactive oxygen species involved under oxygen–hydrocarbon mixture at 425 °C

oxygen–hydrocarbon mixture	hydrocarbon partial pressure/atm	oxygen partial pressure/atm	n	oxygen species
C_3H_8	0.03–0.11[a]	0.15	3.4	O^{2-}
C_3H_8	0.05	0.05–0.30[a]	3.7	O^{2-}
C_3H_6	0.03–0.11[a]	0.15	1.8	O^-
C_3H_6	0.05	0.05–0.30[a]	2.0	O^-

[a] Pressure ranges.

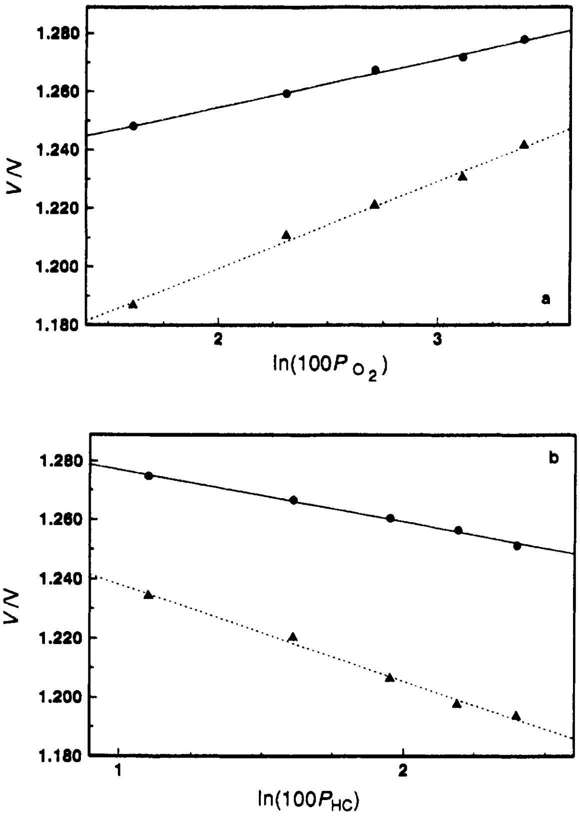

Fig. 9 Potential V under hydrocarbon–oxygen mixture (● C_3H_8, and ▲ C_3H_6) at 425 °C as a function of the logarithm of the partial pressure of (a) oxygen (with the partial pressure of hydrocarbon constant at 5%) and (b) hydrocarbon (with the partial pressure of oxygen constant at 15%)

4. Conclusion

A good correlation is obtained between the work function results and the catalytic tests, showing that the reactivity of propene is much higher than that of propane and explaining the yield limitation often observed in propane oxidation in agreement with a consecutive reaction mechanism $C_3H_8 \xrightarrow{k_1} C_3H_6 \xrightarrow{k_2} CO_x + H_2O$. This simplified model of the oxidation mechanism where K ($K = k_1/k_2$) corresponds to a performance in selectivity, leads to a possible classification of oxydehydrogenation catalysts. A correlation exists also between the two techniques showing that the rate-determining step for the two reactions (propane ODH and propene oxidation) corresponds to the attack of the catalytic surface by the hydrocarbon. Moreover, the work function measurements have shown that propane reacts with the O^{2-} species of the solid and that propene reacts with the O^- species; however, one cannot eliminate the possibility that under catalytic conditions propene can also react with O^{2-} species.

Financial support by ELF-ATOCHEM is gratefully acknowledged.

References

1 M. A. Chaar, D. Patel, M. C. Kung and H. H. Kung, *J. Catal.*, 1987, **105**, 483.
2 M. A. Chaar, D. Patel and H. H. Kung, *J. Catal.*, 1988, **109**, 463.
3 D. Sam, V. Soenen and J. C. Volta, *J. Catal.*, 1990, **123**, 417.
4 K. Seshan, H. M. Swaan, R. H. H. Smits, J. C. van Ommen and J. R. H. Ross, *Stud. Surf. Sci. Catal.*, 1990, **55**, 505.
5 Y-C. Kim, W. Ueda and Y. Moro-Oka, *Stud. Surf. Sci. Catal.*, 1990, **55**, 491.
6 D. Patel, P. J. Andersen and H. H. Kung, *J. Catal.*, 1990, **125**, 132.
7 G. Minow, K. Schnabel and G. Ohlmann, *React. Kinet. Catal. Lett.*, 1983, **22**, 399.
8 F. Harley, Hardman, Lyndhurst, *U.S. Pat.*, 4255284, 1981, to Standard Oil Company.
9 C. Mazzochia, E. Tempesti and C. Aboumrad, *Fr. Pat.*, 89-00522, 1989, to Norsolor.
10 D. B. Dadyburjor, S. S. Jewur and E. Ruckenstein, *Catal. Rev.-Sci. Eng.*, 1979, **19**, 293.
11 H. H. Kung, *Ind. Eng. Chem. Prod. Res. Dev.*, 1986, **25**, 171.
12 V. D. Sokolovskii, *Catal. Rev.-Sci. Eng.*, 1990, **32**, 1.
13 P. M. Michalakos, M. C. Kung, I. Jahan and H. H. Kung, *J. Catal.*, 1993, **140**, 226.
14 M. Ai, *J. Catal.*, 1986, **101**, 389.
15 G. Busca, G. Centi, F. Trifirò and V. Lorenzelli, *J. Phys. Chem.*, 1986, **90**, 1337.
16 G. Centi and F. Trifirò, *Catal. Today*, 1988, **3**, 151.
17 M. Kung and H. Kung, *J. Catal.*, 1991, **128**, 287.
18 G. Centi, F. Trifirò, J. R. Ebner and V. M. Franchetti, *Chem. Rev.*, 1988, **88**, 55.
19 S. T. Oyama, *J. Catal.*, 1991, **128**, 210.
20 M. Merzouri, B. Taouk, L. Tessier, E. Bordes and P. Courtine, *Stud. Surf. Sci. Catal.*, 1993, **75**, 7.
21 A. Guerrero-Ruiz, I. Rodriguez-Ramos, J. L. G. Fierro, V. Soenen, J. M. Hermann and J. C. Volta, *Stud. Surf. Sci. Catal.*, 1992, **72**, 203.
22 A. Corma, J. M. Lopez-Nieto, N. Paredes, M. Perez, Y. Shen, H. Cao, S. L. Suib, *Stud. Surf. Sci. Catal.*, 1992, **72**, 21.
23 S. L. T. Andersson, *Appl. Catal.*, 1994, **112**, 209.
24 G. Centi, *Catal. Today*, 1993, **16**, 5 and 147.
25 J. M. Libre, Y. Barbaux, B. Grzybowska and J. P. Bonnelle, *React. Kinet. Catal. Lett.*, 1982, **30**, 249.
26 Y. Barbaux, J. P. Bonnelle and J. P. Beaufils, *J. Chim. Phys.*, 1976, **73**, 25.
27 B. Grzybowska, Y. Barbaux and J. P. Bonnelle, *J. Chem. Res.*, (S), 1981, 48; *J. Chem. Res.* (M), 1981, 650.
28 Y. Barbaux, A. Elamrani and J. P. Bonnelle, *Catal. Today*, 1987, **1**, 147.
29 C. Mazzochia, C. Aboumrad, C. Diagne, E. Tempesti, J. M. Hermann and G. Thomas, *Catal. Lett.*, 1991, **10**, 181.
30 F. Trifirò and J. Pasquon, *J. Catal.*, 1968, **12**, 412.
31 A. Bielanski and J. Haber, *Catal. Rev. Sci. Eng.*, 1979, **1**, 19.
32 Y. Amenomiya, V. I. Birss, M. Goledzinowski, J. Galuszka and A. R. Sanger, *Catal. Rev.-Sci. Eng.*, 1990, **32**, 163.

Paper 5/01631B; *Received* 14*th March*, 1995